### Title
Estimates of regional natural volatile organic compound fluxes from enclosure and ambient measurements




### Journal
Journal of Geophysical Research, 101(D1)

### ISSN
0148-0227



### Authors
Guenther, Alex
Zimmerman, Patrick
Klinger, Lee
et al.



### Publication Date
1996-01-20

### DOI
10.1029/95jd03006

JOURNAL OF GEOPHYSICAL RESEARCH, VOL. 101, NO. D1, PAGES 1345–1359, JANUARY 20, 1996

# Estimates of regional natural volatile organic compound fluxes from enclosure and ambient measurements

Alex Guenther, Patrick Zimmerman, Lee Klinger, Jim Greenberg, Chris Ennis[1], Kenneth Davis, and Walt Pollock

Atmospheric Chemistry Division, National Center for Atmospheric Research, Boulder Colorado

Hal Westberg and Gene Allwine

Department of Civil and Environmental Engineering, Washington State University, Pullman

Chris Geron

Office of Research and Development, U. S. Environmental Protection Agency, Research Triangle Park, North Carolina

**Abstract.** Natural volatile organic compound (VOC) emissions were investigated at two forested sites in the southeastern United States. A variety of VOC compounds including methanol, 2-methyl-3-buten-2-ol, 6-methyl-5-hepten-2-one, isoprene and 15 monoterpenes were emitted from vegetation at these sites. Diurnal variations in VOC emissions were observed and related to light and temperature. Variations in isoprene emission from individual branches are well correlated with light intensity and leaf temperature while variations in monoterpene emissions can be explained by variations in leaf temperature alone. Isoprene emission rates for individual leaves tend to be about 75% higher than branch average emission rates due to shading on the lower leaves of a branch. Average daytime mixing ratios of 13.8 and 6.6 ppbv C isoprene and 5.0 and 4.5 ppbv C monoterpenes were observed at heights between 40 m and 1 km above ground level the two sites. Isoprene and monoterpenes account for 30% to 40% of the total carbon in the ambient non-methane VOC quantified in the mixed layer at these sites and over 90% of the VOC reactivity with OH. Ambient mixing ratios were used to estimate isoprene and monoterpene fluxes by applying box model and mixed-layer gradient techniques. Although the two techniques estimate fluxes averaged over different spatial scales, the average fluxes calculated by the two techniques agree within a factor of two. The ambient mixing ratios were used to evaluate a biogenic VOC emission model that uses field measurements of plant species composition, remotely sensed vegetation distributions, leaf level emission potentials determined from vegetation enclosures, and light and temperature dependent emission activity factors. Emissions estimated for a temperature of 30°C and above canopy photosynthetically active radiation flux of 1000 μmol $m^{-2}$ $s^{-1}$ are around 4 mg C $m^{-2}$ $h^{-1}$ of isoprene and 0.7 mg C $m^{-2}$ $h^{-1}$ of monoterpenes at the ROSE site in western Alabama and 3 mg C $m^{-2}$ $h^{-1}$ of isoprene and 0.5 mg C $m^{-2}$ $h^{-1}$ of monoterpenes at the SOS-M site in eastern Georgia. Isoprene and monoterpene emissions based on land characteristics data and emission enclosure measurements are within a factor of two of estimates based on ambient measurements in most cases. This represents reasonable agreement due to the large uncertainties associated with these models and because the observed differences are at least partially due to differences in the size and location of the source region ("flux footprint") associated with each flux estimate.

## 1. Introduction

Ambient mixing ratios of volatile organic compounds (VOC) are important variables in the chemistry and transport models used to investigate regional tropospheric oxidant levels. Mixing ratios of many VOC are greatly influenced by variations in surface source strengths due to the short tropospheric lifetimes (minutes to hours) of these compounds. As a result, accurate and highly resolved estimates of fluxes of these highly reactive VOC are required to estimate ambient concentrations. Estimates of VOC fluxes from both anthropogenic and natural sources are limited by a lack of understanding of the processes controlling these fluxes and by the extensive site-specific data required for accurate estimates. Regional and global models of natural VOC emission [e.g., *Lamb et al.*, 1993; *Guenther et al.*, 1995; *Geron et al.*, 1994] have four main components: (1) source distributions, (2) emission potentials, (3) emission algorithms, and (4)

[1]Now at National Oceanic and Atmospheric Administration and Cooperative Institute for Research in Environmental Sciences, Boulder, Colorado.



Paper number 95JD03006.
0148-0227/96/95JD-03006$05.00

estimates of driving variables (e.g., light and temperature). There are significant uncertainties associated with each of these model components. Recent field studies coordinated with the Southern Oxidants Study (SOS) provided an opportunity to evaluate and improve estimates of natural VOC source distributions, emission potentials, and emission algorithms. Investigations at two rural forested locations in the southeastern United States included development and analysis of landscape characterization databases, enclosure measurements of emission rates from the dominant vegetation species, and measurements of ambient VOC mixing ratios up to heights of 1 km above ground level (AGL).

An overview of the field studies is given in section 2. Natural emission modeling techniques for extrapolating leaf-level measurements to the landscape-level surface fluxes required for atmospheric models are described in section 3. Emission model results are given and the role of each model component is considered. Ambient VOC mixing ratios are described in section 4 and are used to evaluate emission model results.

## 2. Field Study Descriptions

Natural VOC fluxes were investigated at two rural locations that are designated as sites in the South East Network for Intensive Oxidant Research (SENIOR) of the Southern Oxidants Study. Field experiments were conducted in June and July of 1990 at the Rural Oxidants in the Southern Environment (ROSE) site in western Alabama (latitude 32.3°N, longitude 88.2°W) and July and August of 1991 at the Southern Oxidants Study - Metter (SOS-M) site in eastern Georgia (latitude 32.5°N, longitude 82.1°W).

### 2.1 Landscape Characterization

The ROSE site is located within the Kinterbish Wildlife Management Area which covers an area of about 160 $km^2$ and is managed by the James River Timber Corporation. On the basis of data supplied by James River Timber, mature forest stands at this site have a canopy height of about 15 m and a leaf foliar density of about 620 g $m^{-2}$ consisting of 85% conifer and 15% hardwood foliage. The forest is dominated by planted loblolly pine *(Pinus taeda)* and includes shortleaf pine *(P. echinata)*, eastern redcedar *(Juniperus virginiana)*, sweetgum *(Liquidambar styraciflua)*, oaks *(Quercus nigra, Q. stellata, Q. phellos, Q. falcata)*, hickory *(Carya* spp.), red maple *(Acer rubrum)*, flowering dogwood *(Cornus florida)*, and sassafras *(Sassafras albidum)*. Shrubs and vines at the site include bayberry *(Myrica)*, kudzu *(Pueraria)*, blackberry *(Rubus)*, and blueberry *(Vaccinium)* species. Oak-pine, oak-hickory, and bottomland hardwood forests dominate the surrounding area. In addition to the species listed above, sugarberry *(Celtis laevigata)*, black tupelo *(Nyssa sylvatica)*, spruce pine *(Pinus glabra)*, and green ash *(Fraxinus pennsylvanica)* are significant components of the forests that surround the site. Data compiled by *Hansen et al.* [1992] indicate that the three-county region surrounding the site is primarily covered by forest lands dominated by *Quercus*, *Pinus*, and *Liquidambar* species. These three genera contribute about 90% of the total leaf biomass within the ROSE site and about 75% in the surrounding area. Fifteen tree species contribute over 95% of the total leaf biomass at the ROSE site and over 85% of the total in the surrounding area. The location of the ROSE site within the surrounding forested and agricultural landscapes is shown in Figure 1 (top).

George Smith State Park and adjacent lands, site of the SOS-M study, covers an area of over 50 $km^2$. The three major natural vegetation communities surrounding the SOS-M site are oak-pine savanna, mesic pine-oak forest, and wet hardwood bottomland. The distribution of woodland and agricultural areas can be seen in Figure 1 (bottom). Three belt transects were used to characterize the composition, successional status, and environmental setting of each vegetation community at the SOS-M site. Measurements included slope, elevation, tree species identification, diameter, height, age, and understory cover.

Oak-pine savanna occurs in upland areas and is dominated by several species of oaks including turkey oak (*Quercus laevis*), sandpost oak (*Q. margaretta*), and bluejack oak (*Q. incana*). Longleaf pine (*Pinus palustris*) and loblolly pine (*P. taeda*) typically are found in these areas as well. The pine-oak forests also occur in uplands and are characterized by a codominance of pine and oak in terms of leaf biomass, though pines comprise most of the woody biomass. These forests include loblolly pine (*P. taeda*), slash pine (*P. elliottii*), bluejack oak (*Q. incana*), and water oak (*Q. nigra*), along with persimmon (*Diospyros virginiana*) and black cherry (*Prunus serotina*). Age structure analyses comparing the oaks and the pines in these forests indicate that the oak are, on average, older that the surrounding pines. This suggests that the oak-pine savanna is a relatively early successional community arising after a disturbance, probably fire, and that the pine-oak forest is a later successional community in the development of upland forests.

The bottomland hardwood forests are highly productive, tall-canopied communities occurring in moist and wet low-lying areas. These are characterized by a wide variety of species which vary in abundance from site to site. The two common trees in these forests are blackgum (*Nyssa* spp.) and red maple (*Acer rubrum*), with cypress (*Taxodium* spp.) in permanently inundated areas. There is a well-developed subcanopy tree layer in these forests that includes red titi (*Cyrilla racemiflora*) and sweetbay (*Magnolia virginiana*).

A land characteristics database was generated using the four visible and near-infrared bands of the Landsat multispectral scanner (MSS) sensor and is referred to in this paper as the LCC-MSS database. The MSS sensor uses broadbands that cover a relatively wide range of wavelengths and has a nominal spatial resolution of 80 m [*Jensen*, 1986]. The Landsat scene for the ROSE site was acquired in 1988 on July 15. The study area consisted of a 41 km × 41 km domain centered on the ROSE site. The image processing methods used included contrast enhancement, band ratios, and principal components transformation. U.S. Geological Survey aerial photos were used to identify known plots of land ("training areas"), and a maximum likelihood technique was used to classify the image. Land surface area was classified as conifer forest, upland deciduous forest, bottomland deciduous forest, or other (primarily agricultural).

For the SOS-M site a time sequence of three scenes (acquired in 1988 on April 14, June 17, and October 7) captured the important components of the seasonal foliar development cycle. The three scenes were spatially registered to each other, and then land use was determined using two techniques, (1)

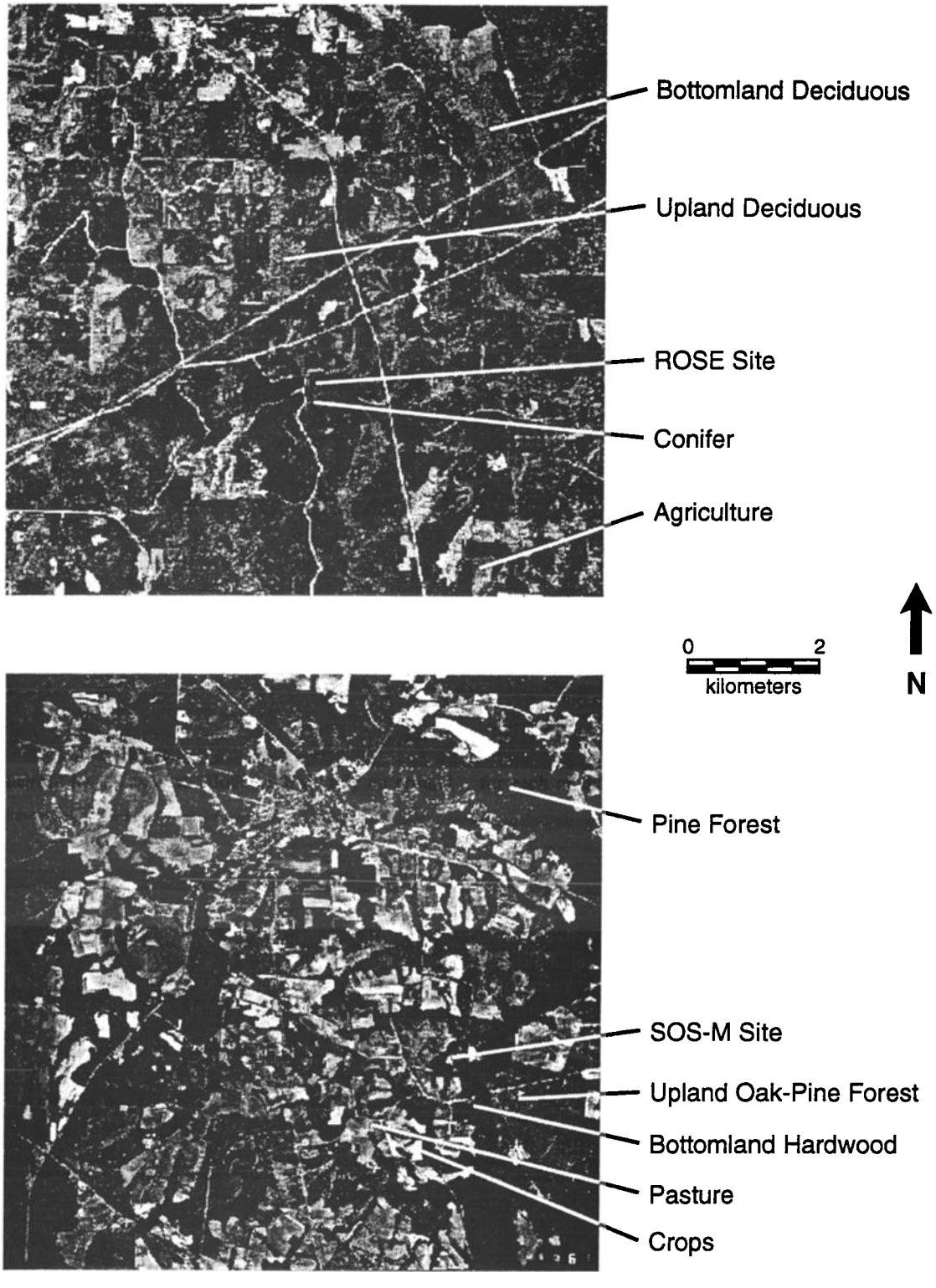


**Figure 1.** Aerial photographs of the (top) Rural Oxidants in the Southern Environment (ROSE) and (bottom) Southern Oxidants Study-Metter (SOS-M) sites.

supervised classification, in which spectral signatures are generated for each land use category using "training areas" and then used as a basis for classifying the rest of the image, and (2) unsupervised classification, in. which spectrally similar pixels are classed together and later identified as a particular land use category by the analyst. Both methods rely on ground truth information gathered from other sources, which here consisted of a color infrared aerial photo obtained on February 16, 1988, and site observations made during the 1991 SOS field study. Image input for each of the classifications consisted of the normalized difference vegetation index (NDVI) for each of the three scenes [*Jensen*, 1986]. This vegetation

index is computed as the ratio of the difference between the near-infrared (NIR) and visible red band (RED) reflectances, divided by the sum of those two reflectances:

$$NDVI = (NIR-RED)/(NIR+RED) \quad (1)$$

The presence of chlorophyll in green vegetation leads to distinctively high values of the NDVI due to chlorophyll's high absorbance in the visible red wavelength region. The NDVI tracks the seasonal pattern of deciduous vegetation, with increasing values in the spring, summertime maxima, and declining values in the fall. Different patterns will occur for coniferous vegetation, cropland, and pastures, forming the basis of the utility of time-sequenced imagery in distinguishing vegetation types. The supervised and unsupervised classification methods are in excellent agreement for the five categories of land use, with the widest discrepancy in the bottomland hardwood category.

### 2.2 Vegetation Enclosure Measurements

VOC emission rates for individual leaves and branches of plants were estimated using field-portable dynamic (open flow) enclosures. Emission rates E were calculated as

$$E = [f(C_o - C_i)]/B \quad (2)$$

where $C_o$ is the concentration in the outlet airstream, $C_i$ is the concentration in the inlet airstream, $f$ is the flow rate into the enclosure, and $B$ is the dry weight foliar mass within the enclosure. Air was passed over an enclosed emission source at a constant rate. Ambient air flowing into an enclosure was pumped through Teflon tubing from locations selected to minimize background concentrations. Uncertainties in $C_o$, $f$, and $B$ result in a total uncertainty of about ±10%. Uncertainties in $C_i$ result in approximately ±0.03 μg C $g^{-1}$ $h^{-1}$ errors in flux estimates which are typically less than 5% of the emission rate for major VOC species. A sufficient flow rate, 1 to 10 L $min^{-1}$ depending on enclosure size, was maintained so that the temperature, humidity, and $CO_2$ mixing ratios within the chamber were similar to ambient conditions.

Individual leaves were sampled with a photosynthesis measurement system (LI-6200, LICOR, Lincoln, NE) with a 1.5 -L cuvette. This commercial system was modified to operate in an open-flow configuration and to allow sampling of inlet and outlet airstreams. Tree branches, shrubs, and ground cover were enclosed with bag enclosures that ranged in volume from 15 to 30 L. The bag enclosures consisted of a rigid aluminum frame covered by a flexible Teflon bag. Bag enclosures were supported by a tripod to minimize contact with the enclosed vegetation.

Leaf temperature, enclosure temperature, relative humidity, photosynthetically active radiation (PAR), and general sampling conditions were recorded for each enclosure measurement. Photosynthesis, transpiration, and stomatal conductance of representative leaves were measured with a LI-6200 system. When an emission rate measurement experiment was completed, the foliage was cut and leaves were dried in an oven and weighed to obtain dry-weight biomass. The ratio of dry-weight leaf biomass to leaf area (measured prior to drying) was determined for each species to provide a conversion factor.

Some enclosure air samples were analyzed for a variety of VOC and used to develop VOC emission potentials. These samples were analyzed by gas chromatography (GC) systems with cryogenic preconcentration using a flame ionization detector (FID) (HP5890, Hewlett Packard, Palo Alto, California) to quantify concentrations and a mass spectrometer detector (MSD) (HP5971, also Hewlett Packard) to identify compounds. The lower detection limit is approximately 10 parts carbon per trillion (pptv C) by volume for a 1-L sample using the GC-FID instrument [see *Greenberg and Zimmerman,* 1984]. This corresponds to a lower bound flux of less than 0.001 μg C $g^{-1}$ $h^{-1}$ for individual VOC. Most samples were analyzed at the field site within 48 hours. Representative samples were stored in stainless steel canisters and transported to a permanent laboratory to provide quality assurance and positive identification of all VOC compounds.

Other enclosure air samples were analyzed only for isoprene, α-pinene, β-pinene, and limonene and used to investigate diurnal emission rate variations. These samples were collected in 20-mL glass syringes and analyzed at the field site using an isothermal gas chromatographic system with a reduction gas detector (Trace Analytical RGD-2). The basic system described by *Greenberg et al.* [1993] was modified to include the following two columns in parallel: a packed column (Unibeads 3S® Alltech Associates, Deerfield, Illinois; 3.2-mm ID × 1-m length) for separating isoprene and a megabore capillary column (DB-1, 1-μm film, 0.53-mm ID × 30-m length, J & W Scientific, Folsom, California) for separating monoterpenes. Oven temperature was kept at 100°C during each sample run. Peak areas were measured with an electronic integrator (HP3390, Hewlett Packard, Palo Alto, California). No preconcentration step was required for this system. The lower detection limit was approximately 5 parts carbon per billion by volume (ppbv C) which corresponds to a lower bound flux of about 0.25 μg C $g^{-1}$ $h^{-1}$ for individual VOC. The responses for isoprene and monoterpenes were compared with compressed gas standards of isoprene and monoterpenes. These standards were calibrated against a National Institute of Standards and Technology certified standard (NIST SRM 1660a 1 ppm propane in nitrogen) on a GC-FID system [*Greenberg and Zimmerman,* 1984].

### 2.3 Ambient Measurements

Ambient air samples were collected in Teflon bags using a whole air sampling unit similar to the system described by *Zimmerman et al.* [1988]. The samplers were attached to the tether line of a helium-filled tethered balloon or to a pulley-mounted line on a tower. Automatic timers on the sampling pumps allowed air samples to be collected simultaneously at two to four heights between 10 m and 1 km above ground level. Sample periods were typically 15 min for the ROSE study and 30 min for the SOS-M study. All ambient air samples were analyzed by the GC-FID and GC-MSD systems described above.

The planetary boundary layer at both sites was characterized using an Advanced Data Assimilation System, tethersondes, and airsondes manufactured by AIR (Boulder, Colorado). The tethersonde provided vertical profiles of wind direction, wind speed, temperature and humidity up to 1 km AGL. Temperature and humidity profiles up to 5 km AGL were measured with airsondes.

Mixing layer heights at ROSE were estimated from Doppler radar measurements [*White and Fairall,* 1991]. Temperature and latent heat fluxes and momentum flux were measured above the forest canopy with instruments deployed on a tower at the ROSE site using the eddy correlation technique (R.T. McMillen, private communication, 1991).

## 3. Enclosure Measurements and Emission Modeling

*Zimmerman* [1979] estimated natural VOC emissions using a simple inventory approach, where an emission rate was multiplied by a leaf biomass factor and a temperature correction factor. Subsequent efforts have used increasingly more accurate and highly resolved input variables and have employed algorithms that provide a more realistic simulation of variations in input variables and the response of emissions to these variables [see *Lamb et al.*, 1993; *Guenther et al.*, 1995; *Geron et al.*, 1994]. An area flux $F$ is estimated from the product of the following three components: foliar mass estimates, emission potentials representative of a specific temperature and PAR, and an emission activity level that accounts for the actual temperature and PAR conditions. Each of the three model components was investigated in this field research program and is described in this section.

### 3.1 Foliar Mass Estimates

Estimates of vegetation distributions around the two field sites were obtained from the following five land cover databases: geoecology, U. S. Department of Agriculture (USDA), eastwide database (EWDB), land cover characteristics-advanced very high resolution radiometer (LCC-AVHRR), and land cover characteristics-multispectral scanner (LCC-MSS). A detailed comparison of these databases is given by *Guenther* [1996]. We focused our comparison on the area covered by the LCC-MSS database which consists of an 80-km × 80-km region surrounding the SOS-M site and a 41-km × 41-km region around the ROSE site. The geoecology [*Olson*, 1980], USDA [*Sheffield and Knight*, 1984], and EWDB [*Hansen et al.*, 1992; *Geron et al.*, 1994], land cover databases contain county-level estimates. The 1681 km$^2$ ROSE region includes portions of three counties, while the 6400 km$^2$ SOS-M region includes all or part of six counties. We have weighted the geoecology, USDA, and EWDB county-level estimates by the fraction of area that each county contributes to a region. The spatial resolution of LCC-MSS, based on LANDSAT-MSS data as described above, and LCC-AVHRR, developed by *Loveland et al.* [1991] using advanced very high resolution radiometer satellite measurements, is 80 m and 1.1 km, respectively. Estimates for individual grids are integrated over each region.

The results compiled in Table 1 show that forest cover estimates range between 66 and 77% around the ROSE site and 58 to 61% at the SOS-M site. These estimates agree quite well, given the different categorization schemes, e.g., some databases grouped areas as mixed forest and cropland, and that the databases represent different years, e.g., the LCC-MSS ROSE database is based on 1988 data while the geoecology and USDA sources represent data compiled between 1970 and 1982. As discussed in the following section, VOC emissions from the foliage of different forest species vary considerably. The emission potentials for different forest types can vary by more than a factor of 5. We have grouped the forests at the two sites into three categories that roughly correspond to the three forest types used in early emission inventory procedures (e.g., Zimmerman 1979). The four methods shown in Table 1 do not agree well at this level of landscape characterization. This is partly due to differences in categorization schemes. The geoecology database greatly underpredicts the amount of coniferous forest because it does not account for the conversion of native mixed forests into pine plantations.

*Guenther et al.* [1994] have shown that three forest categories are not sufficient for natural VOC emission modeling and that the contribution of each plant genus to the total leaf biomass should be estimated when possible. Table 2 contains estimates of foliar mass of the dominant plants at each field site. Over 90% of the total foliar mass at either site can be accounted for by fewer than 10 genera of plants. The

**Table 1.** Relative Contribution of Each Landcover Category to the Total Surface Area at each Study Site in Four Land Cover Characterization Databases

| Landscape | LCC-MSS | USDA | LCC-AVHRR | Geoecology |
|---|---|---|---|---|
| | | *ROSE Site* | | |
| All Forest | 66 | 75 | 74 | 77 |
| Oak-hickory-pine | 24 | 35 | 67 | 62 |
| Pine | 27 | 26 | 4 | 0 |
| Bottomland | 15 | 12 | 3 | 6 |
| Other Forest | 0 | 2 | 0 | 9 |
| Agriculture | 23 | 24 | 24 | 20 |
| Other | 11 | 1 | 2 | 3 |
| | | *SOS-M Site* | | |
| All Forest | 59 \| 61 | 58 | 59 | 60 |
| Oak-pine | 20 \| 22 | 35 | 18 | 0 |
| Pine | 21 \| 22 | 26 | 38 | 0 |
| Bottomland | 15 \| 20 | 12 | 3 | 1 |
| Other Forest | 0 \| 0 | 2 | 0 | 59 |
| Agriculture | 34 \| 38 | 23 | 41 | 27 |
| Pasture | 26 \| 27 | | | |
| Crops | 8 \| 11 | | | |
| Other | 3 \| 5 | 19 | 0 | 13 |

All values are in percent. Abbreviations are as follows: LCC-MSS, land cover characteristics-multispectral scanner; USDA, U.S. Department of Agriculture; LCC-AVHRR, land cover characteristics-advanced very high resolution radiometer; ROSE, Rural Oxidants in the Southern Environment; and SOS-M, Southern Oxidants Study-Metter. LCC-MSS values for SOS-M site on the left result from supervised classification; those on the right are from unsupervised classification.

**Table 2.** Relative Contribution of Each Plant Genus to the Total Foliar Mass at the SOS-M and ROSE sites

| | | SOS-M Foliar Mass g m$^{-2}$ | | | | ROSE Foliar Mass g m$^{-2}$ | | | | EP | |
|---|---|---|---|---|---|---|---|---|---|---|---|
| Genus | Example | EWDB | AVHRR | MSS | GEO | EWDB | AVHRR | MSS | GEO | I | T |
| *Acer* | maple | 22 | 0 | 23 | 0 | 11 | 0 | 10 | 0 | < 0.1 | 0.9 |
| *Carya* | hickory | 3.8 | 0 | 0 | 25 | 13 | 0 | 16 | 52 | < 0.1 | 1.4 |
| *Cornus* | dogwood | 0.8 | 0 | 0 | 0 | 7.3 | 0 | 2.3 | 0 | < 0.1 | < 0.1 |
| *Cyrilla* | red titi | 0 | 0 | 0.3 | 0 | 0 | 0 | 0 | 0 | 14 | 0.1 |
| *Juniperus* | redcedar | 0.1 | 0 | 0 | 0 | 6.1 | 0 | 1.0 | 5.0 | < 0.1 | 0.1 |
| *Liquidambar* | sweetgum | 24 | 0 | 0 | 38 | 52 | 0 | 40 | 5.3 | 71 | 1.3 |
| *Liriodendron* | tulip-tree | 10 | 1 | 0 | 0 | 5.4 | 2 | 6.5 | 0 | < 0.1 | 0.1 |
| *Magnolia* | magnolia | 4.8 | 0 | 0.1 | 38 | 3.0 | 0 | 0.5 | 0 | < 0.1 | 0.5 |
| *Melia* | chinaberry | 0.2 | 0 | 0 | 0 | 0.2 | 0 | 0 | 0 | < 0.1 | < 0.1 |
| *Myrica* | bayberry | 0 | 0 | 0 | 0 | 0 | 0 | 1.1 | 0 | < 0.1 | 2.4 |
| *Nyssa* | gum | 55 | 6 | 50 | 1 | 7.5 | 4 | 8.9 | 3.6 | 13 | 0.6 |
| *Pinus* | pine | 171 | 306 | 140 | 62 | 244 | 280 | 170 | 53 | < 0.1 | 2.0 |
| *Prunus* | cherry | 2.3 | 0 | 4.3 | 0 | 0.9 | 0 | 0.7 | 0 | < 0.1 | < 0.1 |
| *Pueraria* | kudzu | 0 | 0 | 0 | 0 | 0 | 0 | 0.6 | 0 | 97 | < 0.1 |
| *Rubrus* | blackberry | 0 | 0 | 0 | 0 | 0 | 0 | 0.6 | 0 | < 0.1 | 0.2 |
| *Quercus* | oak | 52 | 64 | 80 | 63 | 75 | 58 | 61 | 61 | 68 | 0.1 |
| *Sassafras* | sassafras | 0.1 | 0 | 0 | 0 | 0.4 | 0 | 1.6 | 0 | < 0.1 | < 0.1 |
| *Taxodium* | cypress | 12 | 0 | 0.3 | 1 | 3.0 | 0 | 5.6 | 3.6 | < 0.1 | 2.3 |
| *Ulmus* | elm | 2.7 | 0 | 0 | 0 | 9.4 | 0 | 3.7 | 0 | < 0.1 | 0.1 |
| *Vaccinium* | blueberry | 0 | 0 | 0 | 0 | 0.2 | 0 | 0.6 | 0 | < 0.1 | 0.1 |
| Other | | 9.3 | 0 | 3.9 | 38 | 28 | 0 | 4.1 | 0.3 | | |
| Total | | 370 | 377 | 302 | 266 | 466 | 344 | 335 | 184 | | |

Contributions (in percent) are estimated from databases compiled by eastwide database (EWDB) *[Hansen et al.,* 1992], land cover characteristics-advanced very high resolution radiometer (AVHRR) [*Loveland et al.*, 1991], Geoecology (GEO) [*Olson* 1980], and land cover characteristics-multispectral scanner (MSS). Leaf-level isoprene (I) and monoterpene (T) emission potentials (EP) (μg C g$^{-1}$ h$^{-1}$) were estimated from enclosure measurements at the ROSE and SOS-M sites.

EWDB and LCC-MSS estimates are based on field measurements, while the LCC-AVHRR and geoecology databases do not contain estimates of foliar mass or of the relative proportion of individual plant genera. We estimated foliar mass from land cover data in these two databases using the simple method described by *Guenther et al.* [1994]. The results shown in Table 2 indicate that the estimates for less common trees often differ by more than a factor of 10. Estimates of some of the dominant trees including pines (*Pinus* spp.), sweetgum (*Liquidambar styraciflua*), and gum (*Nyssa* spp.) also differ considerably. Estimates of oak (*Quercus* spp.) foliar mass, the major source of isoprene emission in these forests, are fairly consistent among the four databases.

### 3.2 Emission Potentials

VOC emission potentials (the emission rate at a specified temperature and light intensity) of 30 plant species representing 20 genera were characterized by the measurements described in section 2.2. These plants include all of the species that contribute a significant portion (>0.5%) of the total foliar density at the two field sites. Average isoprene and monoterpene emission rates for each plant genus are shown in Table 2. The emission algorithms described by *Guenther et al.* [1993] were used to normalize emissions to a leaf temperature of 30°C and a leaf-level photosynthetically active radiation intensity of 1000 μmol m$^{-2}$ s$^{-1}$. Conifer trees (*Pinus, Taxodium,* and *Juniperus*) had negligible isoprene emissions and significant monoterpene emissions. Broadleaf trees, vines and shrubs included monoterpene emitters (*Magnolia, Myrica, Carya,* and *Acer* species), isoprene emitters (*Cyrilla, Pueraria,* and *Quercus* species), isoprene and monoterpene emitters (*Nyssa* and *Liquidambar*), and negligible emitters (*Cornus, Melia, Ulmus, Prunus, Rubrus, Vaccinium, Sassafras* and *Liriodendron* species). These observations generally agree with the foliar emission rate measurement data summarized by *Guenther et al.* [1994].

Most foliar emission rate measurement surveys [e.g., *Zimmerman,* 1979] have used whole branch enclosure techniques. This method works well for compounds which are not light dependent but complicates the measurement of isoprene emission rates which are strongly dependent on light conditions [*Guenther et al.*, 1991, 1993]. The shaded leaves on the lower portion of a branch have a considerably lower emission rate than leaves that are in direct sunlight. As a result, the average emission rate for a branch will be lower than the emission rate of a leaf. Early efforts to model regional VOC emissions [e.g., *Lamb et al.,* 1987] did not include canopy radiation transfer models. Instead the canopy

**Table 3.** Comparison of Branch and Leaf Enclosure Measurements of Isoprene Emission Rate Potentials

| Location | Species | Common Name | Branch | Leaf | Ratio |
|---|---|---|---|---|---|
| SOS-M | *Quercus laevis* | turkey oak | 35.4 | 51 | 1.46 |
| ROSE | *Quercus stellato* | post oak | 41.3 | 83.7 | 2.03 |
| ROSE | *Quercus* spp. | all oak | 41.3 | 68.3 | 1.65 |
| ROSE | *Liquidambar styraciflua* | sweetgum | 45.3 | 70.6 | 1.56 |

Emission potentials ($\mu g\ C\ g^{-1}\ h^{-1}$) represent emission rates at 30°C and 1000 $\mu mol\ m^{-2}\ s^{-1}$.

was treated as a big branch so that branch-level measurements could be used and related directly to above canopy PAR levels. Current VOC emission models incorporate canopy light extinction algorithms [e.g., *Lamb et al.*, 1993; *Guenther et al.*, 1995; *Geron et al.*, 1994] and require leaf-level emission potentials since emissions are based on PAR levels calculated for leaves within the forest canopy. The ratio between leaf and branch emission potentials is important because many existing emission rate measurement databases contain branch-level measurements and can be compared with leaf-level measurements only by applying this ratio. We investigated the relationship between branch-level and leaf-level isoprene emission rates for individual branches on several sweetgum (*Liquidambar styraciflua*) and oak (*Quercus* spp.) trees. Table 3 shows that leaf-level isoprene emissions are 75±30% higher than branch-level emissions.

In addition to the hemiterpene isoprene, 15 monoterpene (α-pinene, β-pinene, limonene, sabinene, myrcene, γ-terpinene, tricyclene, α-thujene, camphene, t-ocimene, α-phellandrene, $\Delta^3$-carene, α-terpinolene, α-terpinene, and r-cymene) compounds were emitted from one or more plant species. Three monoterpenes (α-pinene, β-pinene, and limonene) dominated the monoterpene emissions of most plants. Sabinene and myrcene contributed over 15% of emissions from several plants. Almost all of the plant species sampled had only two or three monoterpenes that dominated total monoterpenes emissions. Only bayberry (*Myrica cerifera*) had more than three monoterpenes that each made a significant contribution (>15%) to the total monoterpene emission; in addition to the five monoterpenes listed above, α-terpinene, r-cymene, t-ocimene, and γ-terpinene each contributed 10-15% of total emissions. Tricyclene, α-thujene, camphene, α-phellandrene, $\Delta^3$-carene, and α-terpinolene made small contributions to the total VOC emission of a few plant species.

GC-MSD analyses indicated that a variety of oxygenated VOC compounds are emitted from trees. The compounds observed during this study include low molecular weight compounds such as acetone and methanol and higher weight compounds such as 2-methyl-3-buten-2-ol, 6-methyl-5-hepten-2-one, and n-alkyl aldehydes. The observation of direct emission of the alcohol, 2-methyl-3-buten-2-ol from loblolly pine (*P. taeda*) is the first to demonstrate that it is directly emitted by plants. This compound had previously been identified as an important component of the pheremone of the bark beetle *Ips typographus* [*Lanne et al.*, 1989] and was subsequently reported to be the dominant biogenic VOC in ambient air at Niwot Ridge, Colorado [*Goldan et al.*, 1993]. Goldan et al. conclude that the 2-methyl-3-buten-2-ol at this site is of biogenic origin since ambient concentrations were closely correlated with isoprene, but they did not detect 2-methyl-3-buten-2-ol in vegetation enclosure samples.

### 3.3 Emission Activity Levels

Emission rates of isoprene, α-pinene, β-pinene, and limonene from leaves and branches were measured at intervals of 30 min to 2 hours over periods of 5 to 24 hours at the ROSE site. A total of 136 measurements were made on nine different trees representing three genera (*Pinus, Quercus,* and *Liquidambar*). Typical diurnal emission rate patterns from a representative of each genus are shown in Figure 2. Isoprene emission rates increased with increasing PAR and leaf temperature. Isoprene emission rates associated with PAR levels below 10 $\mu mol\ m^{-2}\ s^{-1}$ were less than 0.1% of maximum rates. Models that simulate these observations are evaluated by *Guenther et al.* [1993].

Monoterpene emissions increased exponentially with increasing leaf temperature. Each 1°C increase in leaf temperature resulted in a 9.4% increase for both α-pinene and β-pinene from both loblolly pine and sweetgum. This result is similar to other recent measurements compared by *Guenther et al.* [1993]. With a 20°C increase from daily minimum and maximum temperatures this results in a factor of 6 increase in hourly emission rates.

### 3.4 Emission Model Results

Using the LCC-MSS database and the emission potentials of *Guenther et al.* [1994], we estimate emission potentials (at a temperature of 30°C and PAR of 1000 $\mu mol\ m^{-2}\ s^{-1}$ on all leaves) of 6.3 mg C $m^{-2}\ h^{-1}$ isoprene and 0.51 mg C $m^{-2}\ h^{-1}$ monoterpenes at the SOS-M site and 7.3 mg C $m^{-2}\ h^{-1}$ isoprene and 0.72 mg C $m^{-2}\ h^{-1}$ monoterpenes at the ROSE site. Emission rate variations due to changes in PAR and temperature simulated by the equations of *Guenther et al.* [1993] are shown for a 2-day period at the ROSE site in Figure 3. Estimated isoprene fluxes range from 0 to 6 mg C $m^{-2}\ h^{-1}$ during the 2-day period. Monoterpene emission rate estimates ranged from 0.35 to 0.8 mg C $m^{-2}\ h^{-1}$. Maximum isoprene and monoterpene fluxes occurred in the afternoon and were higher on the second day by a factor of 2 for monoterpenes and a factor of 3 for isoprene.

## 4. Ambient Measurements

### 4.1 Observed Mixing Ratios

Our analysis of ambient VOC at these rural sites focused on $C_4$ to $C_{10}$ compounds. Isoprene and three monoterpenes, α-pinene, β-pinene, and limonene, were observed in ambient air and were also found in significant quantities in vegetation enclosure samples. Other compounds, primarily benzene, toluene, butane, and pentane, were probably of anthropogenic origin. The results of 22 daytime (0800-1900 LT) sampling periods at the SOS-M site are summarized in Table 4. Data are

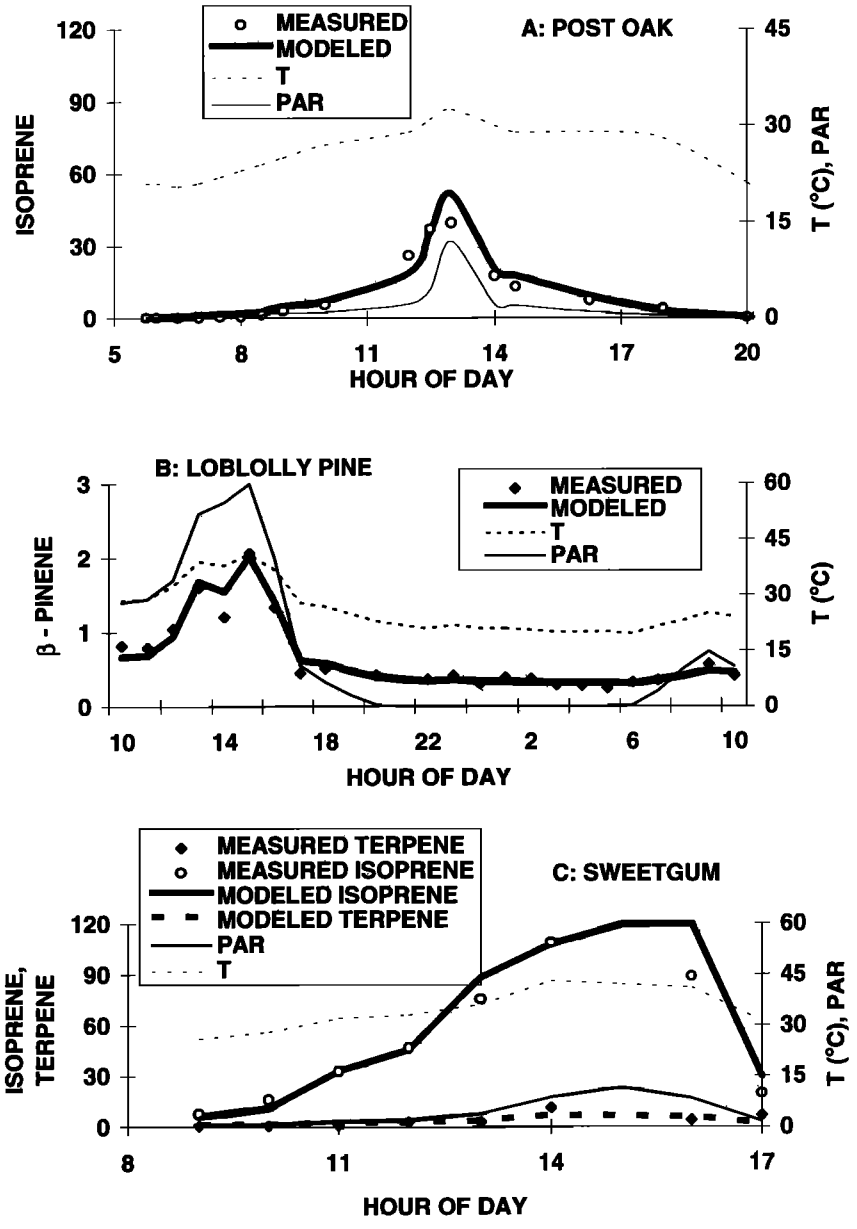


**Figure 2.** Typical observed diurnal isoprene and monoterpene emission (μg C $g^{-1}$ $h^{-1}$) patterns from (a) post oak (b) loblolly pine (c) and sweetgum trees. Leaf temperature T (degrees celsius) and photosynthetically active radiation (PAR) (10 μmol $m^{-2}$ $h^{-1}$) are shown for reference.

shown for surface layer (3 to 120 m AGL) mixing ratio $C_s$ and mixed-layer (200 to 1000 m AGL) mixing ratio $C_m$. The three major biogenic and four anthropogenic VOC resulted in an average total VOC of 38.1 ppbv C in the mixed layer at the SOS-M site. Isoprene contributed about 18% of this total, while α-pinene and β-pinene each contributed about 6%. About half of this total was butane, while toluene, pentane, and benzene contributed the remaining 20%. The impact of each VOC on tropospheric OH concentrations was assessed by normalizing each compound according to reactivity with OH [see *Chameides et al.*, 1992]. The resulting 43.7 ppbv C of "propene-equivalent" carbon for these seven VOC is 63% isoprene, 10% α-pinene and about 20% β-pinene. This simple analysis indicates that these three natural compounds are responsible for a substantial portion of the VOC reactivity with OH at this site. Table 4 also provides a comparison of mixing ratios in the surface and mixed layers. The mean ratio of surface layer mixing ratio to mixed-layer mixing ratio $C_s/C_m$ is greater than 1 for all seven VOC, indicating surface sources. The values of observed $C_s/C_m$ have a very high variability from one sampling period to the next. In addition, the mean value of $C_s/C_m$ for the 20 sampling periods is considerably different than the ratio of mean $C_s$ and mean $C$. This is because the ratio $C_s/C_m$ varied with mixing ratio. For example, $C_s/C_m = 3.9 \pm 1.9$ for $C_m < 1.5$ ppbv C and $C_s/C_m = 0.82 \pm 0.63$ for $C_m > 1.5$ ppbv C for β-pinene. These data demonstrate that mixed-layer average VOC mixing ratios cannot be reliably estimated from surface-layer measurements.

Figure 4 illustrates the vertical structure of the daytime atmospheric boundary layer that is typical of some measurements made at the SOS-M site and most measurements at the ROSE site. The potential temperature, water vapor, and

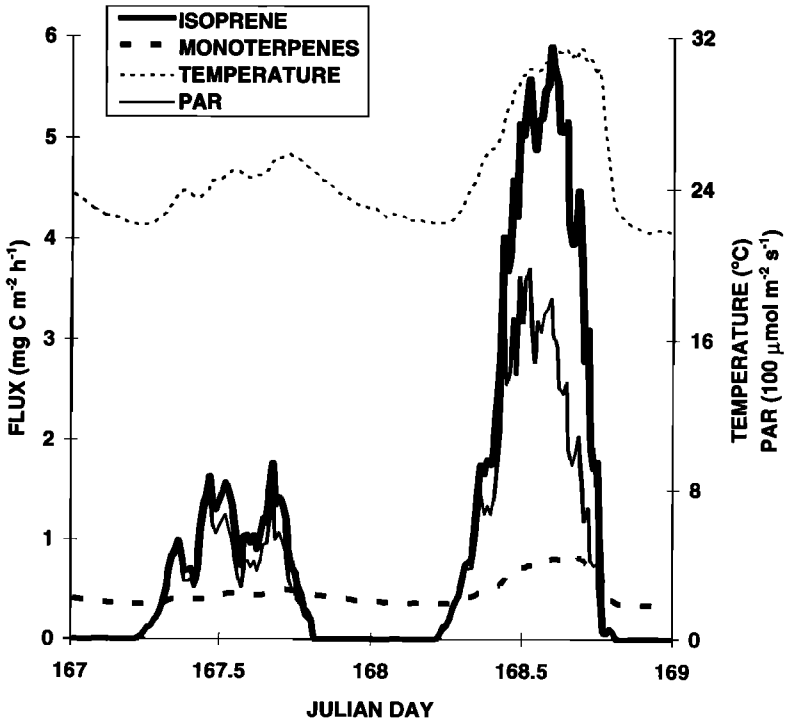


**Figure 3.** Model estimates of area average isoprene and monoterpene fluxes (mg C $m^{-2}$ $h^{-1}$) during July 15 and 16, 1990 at the ROSE site. Temperature (degrees celsius) and PAR (10 µmol $m^{-2}$ $h^{-1}$) are shown for reference.

wind profiles shown in Figure 4 are used to constrain the modeling efforts described below. The mixing ratios of the biogenic hydrocarbons usually decreased with height as is expected for a local surface source of reactive compounds. However, in about 20% of the cases for the SOS-M site and 15% of cases for the ROSE site, biogenic VOC mixing ratios in the mixed layer increased with height (Figure 5). Fluctuations in mixing ratios caused by finite sampling of turbulent eddies in a horizontally homogeneous, well-mixed convective layer are probably too small to explain these profiles. Possible causes of the poorly mixed profiles are locally heterogeneous emissions, cloud circulations and shading, and collapse of the convective layer in the late afternoon.

Figure 6 illustrates the observed vertical distribution of biogenic hydrocarbon mixing ratios in the atmospheric boundary layer above the ROSE and SOS-M sites. These data are summarized in Table 5 and range from about 1 to 70 ppbv C for isoprene and less than 0.1 to about 20 ppbv C for monoterpenes. The median isoprene mixing ratio at the ROSE site was about a factor of 2 higher than at the SOS-M field site. Monoterpene mixing ratios were generally higher at the ROSE site than at the SOS-M site. Monoterpenes were dominated by α-pinene at ROSE, while α-pinene and β-pinene mixing ratios were about the same at SOS-M.

### 4.2 Emission Model Evaluation

**Box model method.** A simplified mixed-layer scalar conservation equation can be written as

$$\frac{\partial C}{\partial t} + U\frac{\partial C}{\partial x} + \frac{\overline{(wc)_{zi}} - \overline{(wc)_o}}{z_i} = S, \qquad (3)$$

**Table 4.** Mean and Standard Deviation of Daytime Ambient VOC Concentrations at the SOS-M Site in the Surface and Mixed Layers

| | Isoprene | α-Pinene | β-Pinene | Butane | Pentane | Benzene | Toluene |
|---|---|---|---|---|---|---|---|
| | | | *Surface Layer* | | | | |
| Mixing ratio, ppbv C | 9.2±7.1 | 3.2±2.5 | 3.0±2.6 | 16.4±23.0 | 2.5±1.6 | 1.1±0.4 | 6.2±17.7 |
| Propene-equivalent, ppbv C | 35.5 | 6.9 | 9.4 | 1.6 | 0.4 | 0.1 | 1.5 |
| | | | *Mixed Layer* | | | | |
| Mixing ratio, ppbv C | 7.0±4.7 | 2.1±1.6 | 2.7±2.8 | 19.2±19.8 | 2.7±2.1 | 1.1±0.4 | 3.3±3.3 |
| Propene equivalent, ppbv C | 27.3 | 4.6 | 8.6 | 1.9 | 0.4 | 0.1 | 0.8 |
| | | | *Comparison of Surface and Mixed Layer* | | | | |
| Mean, $C_s/C_m$ | 1.7±1.1 | 2.3±1.6 | 2.4±2.1 | 3.0±5.0 | 1.2±0.8 | 1.1±0.4 | 3.3±9.3 |
| Mean $C_s$ mean $C_m$ | 1.3 | 1.5 | 1.1 | 0.85 | 0.93 | 1.1 | 1.9 |

Propene-equivalent concentration is normalized by OH reactivity [see *Chameides et al.*, 1992]. A total of 82 samples, 50 in the surface layer and 32 in the mixed layer, were collected during 22 sampling periods.

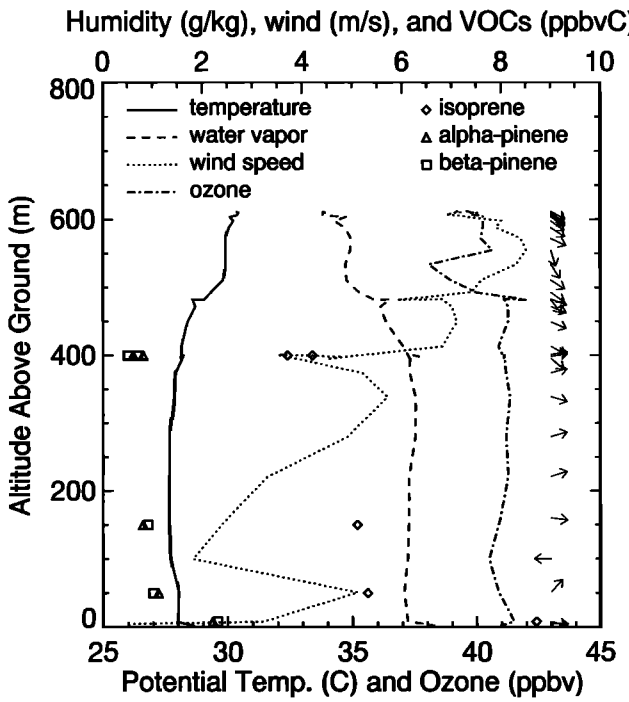


**Figure 4.** Observed vertical variation in potential temperature, water vapor, wind, ozone, isoprene and monoterpene concentrations at 1130 LST on August 4, 1991, at the SOS-M site.

where $C$ is the mean scalar mixing ratio, $U$ is the mean horizontal wind, $t$ is time, $x$ is the horizontal axis aligned with the mean wind, $z_i$ is the height of the mixed-layer capping inversion, $(wc)_{zi}$ and $(wc)_o$ are the turbulent vertical fluxes of scalar $C$ at the inversion and the surface, respectively, and $S$ is a source or sink of the scalar in the mixed layer. This simplified form assumes that turbulent horizontal fluxes and mean vertical advection are negligible and that the vertical flux profile in the mixed layer is linear. These assumptions are all commonly satisfied in the well-mixed convective boundary layer.

We wish to determine the surface flux, so from (3) we write

$$\overline{(wc)_o} = \overline{(wc)_{zi}} + z_i\left(\frac{\partial C}{\partial t} + U\frac{\partial C}{\partial x} + (LC)\right) \quad (4)$$

In our simple box model (BM) estimate of the biogenic hydrocarbon emissions, we assume that the mean mixing ratio has reached a steady state and is homogeneous is space, entrainment flux $(wc)_{zi}$ is negligible, and the hydrocarbons are oxidized primarily by OH and $O_3$ so that the oxidation rate $L$ ($s^{-1}$) is defined as $[k_{OH}\ OH] + [k_{O3}\ O_3]$, where $k_{OH}$ and $k_{O3}$ are reaction rate constants and OH and $O_3$ are mixing ratios of hydroxyl radical and ozone, respectively. Given these assumptions, (4) becomes

$$\overline{(wc)_o} = z_i LC, \quad (5)$$

where $C$ should be interpreted as a mixed-layer average.

We now discuss the limitations of these simplifying assumptions. We can evaluate the errors in our flux estimate which stem from neglecting the entrainment flux $(wc)_{zi}$, time rate of change $z_i(\partial C/\partial t)$, and advection $z_i U(\partial C/\partial x)$ terms in (4). We estimate entrainment using a simple jump model [*Lilly*, 1968]. Since the chemical lifetime of biogenic VOCs is fairly short, we assume that their mixing ratio is zero above the boundary layer. The jump in VOC mixing ratio across the planetary boundary layer top is then roughly the mean boundary layer mixing ratio. The entrainment flux is given by the product of the jump in mixing ratio and the mixed-layer growth rate (typically, about 0.05 m $s^{-1}$ during the day). Since entrainment dilutes the mixed layer, neglecting entrainment in the box model causes a systematic underestimate of the surface flux. This underestimate is, at most, about 1 mg C $m^{-2}$ $h^{-1}$ for isoprene, 0.2 mg C $m^{-2}$ $h^{-1}$ for α-pinene, and 0.1 mg C $m^{-2}$ $h^{-1}$ for β-pinene. Nonzero mixing ratios of biogenic VOC above the boundary layer will minimize this underestimate.

We cannot distinguish the mixing ratio time rate of change $z_i(\partial C/\partial t)$, from advection $z_i U(\partial C/\partial x)$ using these observations, but we can estimate the magnitude of the sum of these terms by observing the evolution in the mean mixing ratio profile over time for days with more than one balloon profile. We expect the mixing ratio to increase over the course of the day, neglecting advection. This would mean that the box model, which assumes steady state, again underestimates the surface fluxes. The observations, however, show significant but random trends in the mixed-layer average mixing ratio over the course of the day. This indicates that the steady state approximation is, on the average, reasonable and that advection, random in sign, is the dominant term. The mean time rate of change in mixing ratio for both experiments is about 0 ± 1 ppbv C $h^{-1}$ for isoprene and 0 ± 0.5 ppbv C $h^{-1}$ for α- and β-pinene. Multiplied by a typical 1000-m $z_i$, this implies an uncertainty of ± 0.4 mg C $m^{-2}$ $h^{-1}$ isoprene and ±0.2 mg C $m^{-2}$ $h^{-1}$ α- and β-pinene in the box model surface flux estimates.

Next we analyze the degree of uncertainty in the inputs to our box model flux estimate (5). The largest source of

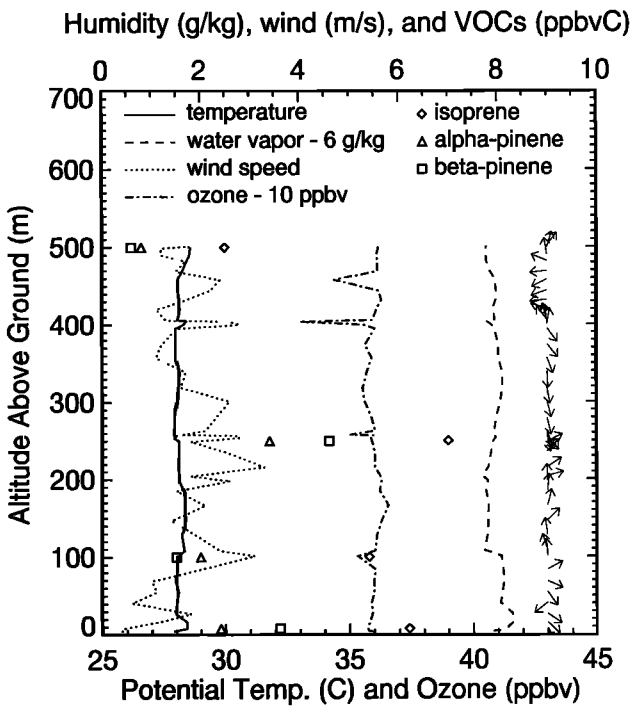


**Figure 5.** Observed vertical variation in potential temperature, water vapor, wind, ozone, isoprene and monoterpene concentrations at 1230 LST on August 11, 1991 at the SOS-M site.

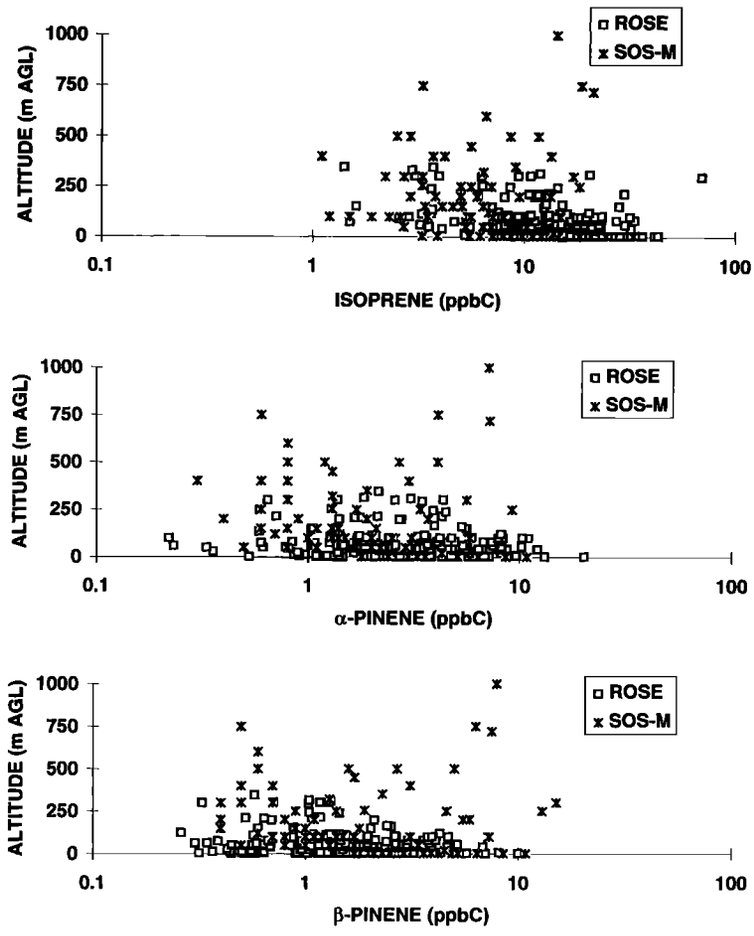


**Figure 6.** Observed (top) isoprene, (middle) a-pinene, and (bottom) b-pinene mixing ratios at the ROSE and SOS-M sites.

uncertainty is the OH concentration needed to estimate the chemical loss rate $L$. To estimate the chemical loss rate $L$, we used the OH and ozone reaction rate coefficients reported by *Atkinson* [1990] and the measured ozone mixing ratios. The uncertainty in the actual OH concentration at these sites is at least 50%. For example, *Montzka et al.* [1993] recommend $2 \times 10^6$ molecules $cm^{-3}$ for the ROSE site, *Chameides et al.* [1992] set OH concentrations at $4 \times 10^6$ molecules $cm^{-3}$ for an analysis that includes our ROSE data, and *Jacob et al.* [1993] use an OH concentration of $6 \times 10^6$ molecules $cm^{-3}$ in a comparison of the hydrocarbon mixing ratios we measured at the ROSE site. We use a maximum OH concentration of $4 \times$

**Table 5.** Comparison of Predicted and Observed Hydrocarbon Concentrations

| | Isoprene | | Monoterpenes | |
|---|---|---|---|---|
| | Observed | Predicted | Observed | Predicted |
| | | *ROSE n=105* | | |
| Mean ± sd | 13.8±9.0 | 13.3±9.5 | 5.0±3.7 | 4.0±2.4 |
| Minimum | 1.4 | 0.8 | <0.1 | 0.7 |
| Median | 12.5 | 10.5 | 4.4 | 3.2 |
| 75th percentile | 18.7 | 17.1 | 6.5 | 5.8 |
| Maximum | 69.4 | 37.4 | 18.9 | 10.6 |
| | | *SOS-M, n=65* | | |
| Mean ± sd | 6.6±4.7 | 11.6±6.3 | 4.5±4.7 | 3.1±1.3 |
| Minimum | 1.4 | 1.3 | <0.1 | 0.8 |
| Median | 5.4 | 11.6 | 2.8 | 3.0 |
| 75th percentile | 7.8 | 16.2 | 4.6 | 3.7 |
| Maximum | 21.1 | 30.7 | 22.1 | 7.6 |

The predicted concentrations are based on fluxes estimated using the LCC-MSS landscape data and emission potentials from *Guenther et al.* [1994]. All samples were collected between 0800 and 1700 LST at heights above 40 m above ground level. Concentrations are in parts per billion of carbon.

$10^6$ molecules $cm^{-3}$ and the OH diurnal variation described by *Lu and Khalil* [1991]. *Jacob et al.* [1993] note that the few direct measurements of OH concentrations in rural air tend to be lower than those computed from photochemical models. This is probably because the models underestimate OH sinks such as oxygenated VOC. This 50% uncertainty in OH concentration translates directly into a 50% uncertainty in the box model flux estimates. Any error is likely to be systematic.

Our estimates of the mean mixing ratio $C$ added some uncertainty. For any one biogenic VOC profile the typical standard deviation of the mean mixing ratio was approximately 25% of the mean. We fit a reasonable vertical profile (*Chameides et al.* [1992] below 150 m and *Moeng and Wyngaard* [1989] for the rest of the mixed layer) to each observed mixing ratio profile and computed the vertical average of the fit to obtain $C$. Since this vertical variability is accounted for, the 25% standard deviation of the mean is an overestimate of the uncertainty in $C$. The uncertainty in $C$ is likely to be random in sign from one profile to the next.

Another source of uncertainty in (5), are the estimates of $z_i$ from boundary layer radar during ROSE [*White and Fairall*, 1991] and airsonde and tethersonde profiles during SOS-M. The $z_i$ estimates typically have an uncertainty of about 15%, and errors are likely to be random.

We conclude that the flux estimated by equation (5) is subject to a total random uncertainty of about 25% due to the roughly 20% and 15% random, independent uncertainty in our estimates of $C$ and $z_i$, respectively. OH introduces an approximately 50% uncertainty in the flux and is likely to be a systematic error whose sign we do not know. Direct OH measurements will resolve this issue.

**Mixed-layer gradient estimates.** The isoprene and monoterpene mixing ratio profiles were also used to estimate surface fluxes using the mixed-layer gradient MLG technique. This technique assumes that boundary layer mixing is dominated by convective turbulence and that boundary layer conditions evolve slowly compared to the convective turnover time $z_i/w_*$ of about 10 min (9.4 ± 3.3 min for SOS-M and 10.0 ± 4.0 min for ROSE), where $w_*$ is the convective velocity scale, typically about 1-2 m $s^{-1}$ during midday. These assumptions, which we call the mixed-layer assumptions, require that all the terms in the vertical derivative of (3) are small and that the flux profile in the mixed layer is linear (K. J. Davis and D. H. Lenschow, Scalar profiles and fluxes in the mixed-layer, submitted to *Boundary-Layer Meteorology*, 1995). The technique, therefore, is not affected by vertically homogeneous horizontal advection, $\delta/\delta z[U(\delta C/\delta x)] \rightarrow 0$, or time dependence in the mean mixing ratio, $\delta/\delta z[(\delta C/\delta t)] \rightarrow 0$, and it accounts for entrainment. Since this technique does not depend directly on scalar reactivity for the flux estimate, it is relatively insensitive to uncertainties in the OH concentration. In principle, therefore this technique uses more robust assumptions than the box model.

This method does assume that the scalar of interest is conserved on the timescale of convective mixing. Table 6 shows estimates of the lifetimes of isoprene and monoterpenes for these experiments. The roughly 1-hour lifetimes are fairly long compared with the 10-min convective turnover time, but some overestimates of the fluxes may result from not accounting for this reactivity. Using the very simple argument of *Davis et al.* [1994], we estimate that for a mean mixed-layer isoprene mixing ratio of 7.5 ppbv C, a surface flux of 4 mg C $m^{-2}$ $h^{-1}$, a 10-min convective turnover time, and a 40-min isoprene lifetime, the MLG technique may overestimate the surface flux by as much as 25%.

**Table 6.** Comparison of Mean and Standard Deviation of the Mean Fluxes

| | MLG | BM | Model | MLG/BM | $\tau(h)$ |
|---|---|---|---|---|---|
| | | *ROSE Site* | | | |
| Isoprene | 3.9±2.9 | 6.9±1.0 | 4.8±0.5 | 0.57 | 0.69 |
| α-pinene | 1.5±0.9 | 1.1±0.16 | | 1.4 | 0.91 |
| β-pinene | 0.70±0.49 | 0.58±0.09 | | 1.2 | 0.82 |
| Terpenes | 2.2±1.3 | 1.7±0.22 | 0.80±0.05 | | |
| | | *SOS-M Site* | | | |
| Isoprene | 3.0±2.4 | 4.0±1.1 | 5.6±0.8 | 0.75 | 0.69 |
| α-pinene | 1.9±1.4 | 1.1±0.3 | | 1.7 | 0.91 |
| β-pinene | 1.2±1.7 | 1.1±0.4 | | 1.1 | 0.82 |
| Terpenes | 3.1±3.0 | 2.2±0.7 | 0.72±0.08 | | |

All fluxes (in mg C $m^{-2}$ $h^{-1}$) were estimated using mixed layer concentration gradients (MLG), mixed layer mean concentrations in the box model (BM) approach, and emission model (model) estimates. The emission model estimates use the LCC-MSS data and emission potentials from *Guenther et al.* [1994]. The 20 sets of concentration data collected at the ROSE site were associated with mid-day conditions with minimum cloud cover and temperatures of 30.8±0.7°C and photosynthetically active radiation (PAR) of 1262±103 μmol $m^{-2}$ $s^{-1}$. The nine sets of concentration data collected at the SOS-M site were associated with mid-day conditions with minimum cloud cover and temperatures of 33.3±1.1°C and PAR of 1325±154 μmol $m^{-2}$ $s^{-1}$. The lifetime of each compound $\tau(h)$ assumes a maximum OH concentration of 4 x $10^6$ molecules $cm^{-3}$ and an ozone concentration of 40 ppb.

There is some uncertainty in accounting for the displacement height of the forest canopy [*Stull* 1988]. We have chosen to neglect displacement height for these estimates. This may cause, at the extreme, about a 30% overestimate in the fluxes calculated at these sites.

In practice, the MLG technique depends on accurate measurements of small vertical gradients in mixing ratio, while the box model is based on the more robust measurement of the mean mixing ratio. Most of the ROSE and SOS-M profiles were collected over 15 to 30 min, long enough to average across the advection of at most a few mixed-layer thermals. This limited sampling results in significant uncertainty in our observations of the vertical mixing ratio differences. This uncertainty translated directly into uncertainty in our surface flux estimates. *Davis* [1992] discusses the sampling error in a vertical mixing ratio difference. For a 30-min sampling time and typical values observed during ROSE and SOS-M ($(wc)_o$ = 4 mg C $m^{-2}$ $h^{-1}$, $U$ = 4 m $s^{-1}$, $z_i$ = 1000 m, and $w_*$ = 1.5 m $s^{-1}$), the error variance in the vertical mixing ratio difference, if the observations at the two levels are independent, should be of the order of 2.5 ppbv C compared to an expected difference between 100 and 500 m of about 2.0 ppbv C. However, because eddies in the convective boundary layer are large, vertical coherence between the two levels as computed by *Davis* [1992] from dual-aircraft observations may reduce the error in the mixing ratio difference to as little as order 0.5 ppbv C. The result would be roughly 25% uncertainty in the surface flux estimates derived from two mixing ratio observations.

While this discussion is somewhat helpful, the observations show that the actual variability in mixing ratio differences is probably larger than can be accounted for by sampling error. Violations of the mixed-layer assumptions

could be causing significant variability in the measured vertical gradients and the resulting flux estimates. The most likely violations of the mixed-layer assumptions are vertically varying horizontal advection caused by heterogeneity in surface fluxes on the scale of one to a few kilometers and irregular mixing caused by extensive convective cloud activity. We have attempted to eliminate periods where cloud activity may perturb boundary layer mixing. We cannot evaluate an expected magnitude for errors in the surface flux measurements due to surface heterogeneity with the current set of observations.

Flux estimates from ROSE are presented by *Davis et al.* [1994]. The profiles which remained after meteorological screening for convective mixing showed some evidence of variability which could be indicative of heterogeneous emissions. There was more profile variability, for example, than existed in a similar data set collected in an Amazon forest preserve [see *Davis et al.*, 1994]. The SOS-M results, presented here, show considerable evidence of poorly mixed profiles, even after screening the data for conditions without strong convective mixing. Figure 1 shows the landscapes around the two sites. It seems reasonable from the varying landuse seen in these aerial photos that the flux estimates at the SOS-M site are influenced from more spatial heterogeneity than the ROSE site, that variability exists at both sites on the scale of one to a few kilometers needed to disturb the mixed-layer assumptions, and that the pattern of heterogeneity is fairly random with respect to wind direction at both sites. We proceed therefore assuming that any variability in the vertical profiles caused by heterogeneous emissions is random and that our results averaged over all profiles are meaningful.

**Comparison of box model and mixed-layer gradient methods.** Fluxes estimated using the BM and MLG methods are compared in Table 6. It should be noted that emissions estimated using the MLG technique represent fluxes from a horizontal fetch of the order of several kilometers, while fluxes estimated by the BM method represent a horizontal fetch of the order of tens of kilometers.

The total midday biogenic VOC flux estimated by the MLG method is about 6 mg C $m^{-2}$ $h^{-1}$ at both sites, while the BM method estimates total VOC fluxes of about 6 mg C $m^{-2}$ $h^{-1}$ at SOS-M and 8.6 mg C $m^{-2}$ $h^{-1}$ at ROSE. Monoterpene fluxes calculated by the MLG method contribute 36% to 50% of the total flux at both sites. The BM method estimates that monoterpenes contribute 20% of the total flux at the ROSE site and 35% at the SOS-M site. The MLG estimates are lower for isoprene (25 to 43%), higher for α-pinene (36 to 72%), and slightly higher for β-pinene (9 to 20%) relative to the BM estimates at the two sites. The similarity at both sites in the comparison of the techniques is very encouraging. Although we cannot rule out coincidence, especially given the large variability in individual flux estimates present in both techniques, the mean fluxes obtained appear to be meaningful and reproducible.

It is interesting to note that, as shown in Table 6, the most reactive (with respect to OH) of these three compounds, isoprene, has consistently lower flux estimates with the MLG technique (relative to the BM estimates), while for the least reactive compound, α-pinene, the MLG technique predicts the highest relative fluxes. The systematic errors which we have identified due to neglecting entrainment in the BM and neglecting scalar reactivity and displacement height in the MLG technique could only help resolve the discrepancy in terpene fluxes since they result in increasing the BM flux estimates and decreasing the MLG flux estimates. If OH is overestimated in the box model, this would help resolve the discrepancy in isoprene fluxes but would exacerbate the comparison of terpene fluxes. Another possible explanation is the mismatch in flux footprints. The range of the MLG footprint is a few kilometers, while the BM footprint is over 10 km. The density of monoterpene emitters decreases beyond a few kilometers fetch due to the high density of pine trees near the center of each site. Since the BM is sensitive to a larger footprint, this nearby concentration of pine trees would result in higher monoterpene and lower isoprene fluxes estimated by the MLG technique.

**Comparison with emission model estimates.** Best estimates of isoprene and monoterpene emission rates were calculated using the emission potentials of *Guenther et al.* [1994], the light and temperature algorithms of *Guenther et al.* [1993], the canopy model of *Guenther et al.* [1995], and the LCC-MSS landscape characterization data. Figure 7 compares observed mixing ratios with values estimated from predicted fluxes using the one-dimensional diffusion and chemistry model of *Chameides et al.* [1992] from the surface to 150 m AGL and the mixed-layer gradient model of *Moeng and Wyngaard* [1989] to estimate decreases in height from 150 m to the top of the mixed layer. The emission model domain extends about 20 to 40 km from the sites where ambient mixing ratios were measured so that predicted mixing ratios should be generally representative of observed mixing ratios in the mixed layer. For the sampling periods selected for mixed-layer analysis ($n$=20 for ROSE and $n$=9 for SOS-M), typically about 60% of the predicted mixing ratios are within a factor of 2 of observed mixing ratios and 95% are within a factor of 3. The best agreement was observed for predicted monoterpene mixing ratios at the ROSE site, 90% are within a

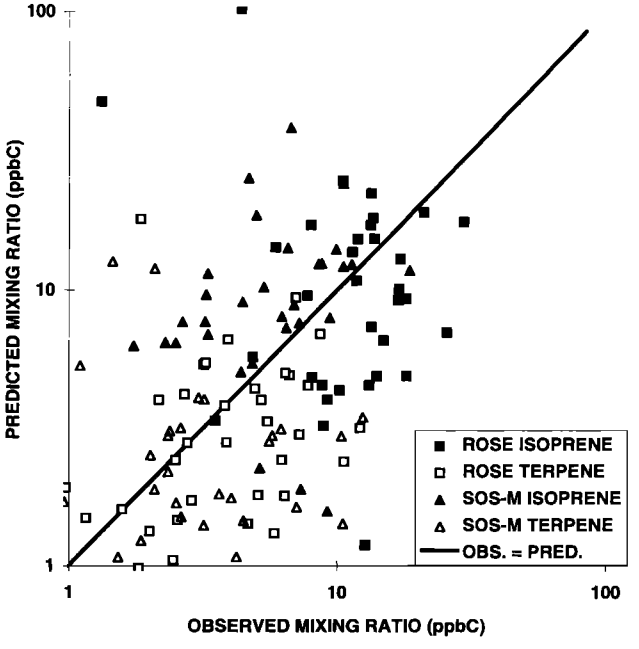


**Figure 7.** Comparison of predicted and observed isoprene and monoterpene mixing ratios at the ROSE and SOS-M sites. The predicted values are based on fluxes estimated using the land cover characteristics-multi spectral scanner landscape data and emission potentials from *Guenther et al.* [1994].

**Table 7.** Area-Average Emission Rate Potentials

| | ROSE | | SOS-M | |
|---|---|---|---|---|
| | Isoprene | Terpene | Isoprene | Terpene |
| | | *Ambient* | | |
| Box model | 6.6±1.1 | 1.8±0.2 | 3.2±0.7 | 1.4±0.2 |
| ML gradient | 6.7±3.9 | 2.3±1.1 | 1.5±1.2 | 2.0±1.7 |
| | | *Enclosure* | | |
| LCC-MSS | 3.8 | 0.72 | 3.3 | 0.51 |
| EWDB | 4.8 | 0.58 | 3.1 | 0.36 |
| LCC-AVHRR | 2.1 | 0.85 | 2.4 | 0.93 |
| Geoecology | 2.4 | 0.29 | 3.7 | 0.49 |

Emission potentials are in mg C $m^{-2}$ $h^{-1}$ at a temperature of 30°C and PAR of 1000 μmol $m^{-2}$ $s^{-1}$ and have been adjusted to account for canopy shading. Flux estimates, mean, and standard deviation of the mean, based on ambient concentrations are representative of an area of 400 to 1600 $km^2$ for the box model estimates and 25 to 100 $km^2$ for the mixed-layer gradient (MLG) estimates. The EWDB, LCC-MSS, LCC-AVHRR, and geoecology (see Table 2) flux estimates use the emission potentials of *Guenther et al.* [1994] and are averaged over a 1681 $km^2$ area surrounding the ROSE site and a 6400 $km^2$ area surrounding the SOS-M site. The EWDB estimates were calculated using the canopy model described by *Geron et al.* [1994], while the other estimates were based on the canopy model used by *Guenther et al.* [1995].

factor of 2, while the worst agreement was observed for monoterpene mixing ratios at the SOS-M site, only 78% are within a factor of 3. A statistical comparison of observed and predicted mixing ratios is given in Table 5. The predicted range and variability are similar to the observed for both isoprene and monoterpenes. The predicted average and median values are within 30% of observed values in each case except that predicted isoprene mixing ratios are a factor of 2 higher at the SOS-M site. We consider this to be reasonably good agreement since a factor of 2 random difference due to heterogeneity of sources within this region can be expected. This uncertainty could be substantially reduced by matching flux estimates with specific flux footprints.

Estimates of area-averaged emission potentials for isoprene and monoterpenes are given in Table 7. All estimates represent a temperature of 30°C and PAR of 1000 μmol $m^{-2}$ $s^{-1}$ and account for the effects of canopy shading. The LCC-MSS emission model isoprene flux estimates are 42% lower and 3% higher than the BM estimates at the ROSE and SOS-M sites respectively. Emission model estimates of monoterpene flux estimates were 60% lower than the BM estimates at both sites. Given the large variability in the observed mean ambient mixing ratio, in the landscape characterization databases, and in the differences in the source region represented by the different techniques, there is reasonably good agreement between these estimates.

## 5. Summary and Conclusions

The results of field measurements at two forested sites in the southeastern United States provide a database for improving and evaluating biogenic VOC emission models. An analysis of land cover characteristics databases shows that there is a variety of techniques that can be used to determine total forested area but that accurate estimates of plant species composition require field measurements of vegetation distributions. Databases that have detailed landscape types, e.g., oak and pine forest, but no species composition estimates can lead to a factor of 2 or more difference in emission estimates.

Uncertainties in emission potentials contribute a large part of the overall uncertainty in emission model estimates. Isoprene emission rates for individual leaves tend to be about 75% higher than emission rates averaged over an entire branch due to shading on the lower leaves of a branch. Emission potentials of VOC compounds other than isoprene and monoterpenes are especially uncertain but may contribute significantly to the total flux.

Average daytime mixing ratios of 13.8 and 6.6 ppbv C isoprene and 5.0 and 4.5 ppbv C monoterpenes were observed at the two sites. Together, these biogenic compounds contain about 35% of the total carbon in nonmethane VOC and over 90% of the VOC reactivity with OH.

VOC fluxes estimated from ambient mixing ratios using a box model technique and a mixed-layer gradient technique agree within a factor of 2. Fluxes estimated by extrapolating enclosure measurements (emission model) and based on ambient mixing ratios (box and gradient models) were within a factor of 2 in most cases and within a factor of 3 in over 90% of all cases. Emission model estimates for isoprene were within 5% of those based on ambient mixing ratios at one site and 42% lower at the other site. Monoterpene emissions estimated by the emission model were about 60% lower than observed at both sites. A qualitative assessment suggests that higher monoterpene flux estimates should be expected from the ambient mixing ratio data which represent fluxes averaged over a smaller area surrounding the site. These results show that emission models can provide reasonable estimates of ambient isoprene and monoterpene mixing ratios. This comparison can be made with more certainty by obtaining (1) accurate estimates of the source region (flux footprint) associated with each ambient mixing ratio profile, (2) a better understanding of when the mixed-layer assumptions are valid, and (3) more accurate estimates of the variables used to estimate fluxes from ambient measurements (e.g., OH concentration).

**Acknowledgments.** This research was partially supported by the U. S. Environmental Protection Agency, Research Triangle Park, North Carolina, under Interagency Agreement grant DW49934973-01-0, the National Oceanic and Atmospheric Administration, Boulder Colorado, and the Southern Oxidants Study (SORP-EE/SERON). The National Center for Atmospheric Research is sponsored by the National Science Foundation. Surface meteorology and ozone measurements were provided by R. McMillen (ROSE) and Y. Lee (SOS-M). We thank William Bradley, Kevin Guenther, Marisa Kadavanich, Rick Lowe, and Mary Wildermuth for assistance in field measurements.

## References

Atkinson, R., Gas-phase tropospheric chemistry of organic compounds: a review, *Atmos. Environ., 24A*, 1-41, 1990.

Chameides, W., et al., Ozone precursor relationships in the ambient atmosphere, *J. Geophys. Res., 97*, 6037-6055, 1992.

Davis, K.J., Surface fluxes of trace gases derived from convective-layer profiles. *Publ. NCAR/CT-139*, NCAR, Boulder, Colorado, 1992.

Davis, K.J., D.H. Lenschow and P.R. Zimmerman, Biogenic nonmethane hydrocarbon emissions estimated from tethered balloon observations, *J. Geophys. Res., 99*, 25,587-25,598, 1994.

Geron, C., A. Guenther, and T. Pierce, An improved model for estimating emissions of volatile organic compounds from forests in the eastern United States, *J. Geophys. Res., 99*, 12,773-12,792, 1994.

Goldan, P., W. Kuster, F. Fehsenfeld, and S. Montzka, The observation of a $C_5$ alcohol emission in a North American pine forest, *Geophys. Res. Lett., 20*, 1039-1042, 1993.

Greenberg, J.P., and P.R. Zimmerman, Nonmethane hydrocarbons in remote tropical, continental, and marine atmospheres, *J. Geophys. Res., 89*, 4767-4778, 1984.

Greenberg, J., P. Zimmerman, B. Taylor, G. Silver, and R. Fall, Sub-parts per billion detection of isoprene using a reduction gas detector with a portable gas chromatograph, *Atmos. Environ., Part A, 27A*, 2689-2692, 1993.

Guenther, A., Seasonal and spatial variations in natural volatile organic compound emissions, *Ecol. Appl.*, (in press), 1996.

Guenther, A., R. Monson, and R. Fall, Isoprene and monoterpene emission rate variability: Observations with eucalyptus and emission rate algorithm development, *J. Geophys. Res., 96*, 10,799-10,808, 1991.

Guenther, A., P. Zimmerman, P. Harley, R. Monson, and R. Fall, Isoprene and monoterpene emission rate variability: Model evaluation and sensitivity analysis, *J. Geophys. Res., 98*, 12,609-12,617, 1993.

Guenther, A., P. Zimmerman, and M. Wildermuth, Natural volatile organic compound emission rate estimates for U.S. woodland landscapes, *Atmos. Environ., 28*, 1197-1210, 1994.

Guenther, A., et al., A global model of natural volatile organic compound emissions, *J. Geophys. Res., 100*, 8873-8892, 1995.

Hansen, M., T. Frieswyck, J. Glover, and J. Kelly, The eastwide forest inventory database: User's manual, *Gen. Tech. Rep., NC-151*, 48 pp., U.S. Dep. of Agric., Forest Serv., St. Paul Minn., 1992.

Jacob, D., et al., Simulation of summertime ozone over North America, *J. Geophys. Res., 98*, 14,797-14,816, 1993.

Jensen, J., *Introductory Digital Image Processing*, 379 pp., Prentice-Hall, Englewood Cliffs, N.J. 1986.

Lamb, B., A. Guenther, D. Gay, and H. Westberg, A national inventory of biogenic hydrocarbon emissions, *Atmos. Environ., 21*, 1695-1705, 1987.

Lamb, B., D. Gay, H. Westberg, and T. Pierce, A biogenic hydrocarbon emission inventory for the U.S.A. using a simple forest canopy model, *Atmos. Environ., Part A, 27A*, 1673-1690, 1993.

Lanne, B., P. Ivarsson, P. Johnsson, G Bergström, and A. Wassgren, Biosynthesis of 2-methyl-3-buten-2-ol, a pheremone component of *Ips typographus* (Coleoptera: Scolytidae), *Insect Biochem., 19*, 163-167, 1989.

Lilly, D.K., Models of cloud-topped mixed layers under a strong inversion, *Q. J. R. Meteorol. Soc., 94*, 292-309, 1968.

Loveland, T., J. Merchant, D Ohlen, and J. Brown, Development of a land-cover characteristics database for the coterminous U.S., *Photogramm. Eng. Remote Sens., 57*, 1453-1463, 1991.

Lu, Y., and M. Khalil, Tropospheric OH: Model calculations of spatial, temporal, and secular variations, *Chemosphere, 23*, 397-444, 1991.

Moeng, C., and J. Wyngaard, Evaluation of turbulent and dissipation closures in second order modeling, *J. Atmos. Sci., 46*, 2311-2330, 1989.

Montzka, S., M. Trainer, P. Goldan, W. Kuster, and F. Fehsenfeld, Isoprene and its oxidation products, methyl vinyl ketone and methacrolein, in the rural troposphere, *J. Geophys. Res., 98*, 1101-1111, 1993.

Olson, R. Geoecology: A county-level environmental data base for the coterminous United States, Environ. Sci. Div., Oak Ridge *Nat. Lab., Publ. 1537*, Oak Ridge, Tenn., 1980.

Sheffield, R., and H. Knight, Georgia's Forest, *USDA Forest Serv. Resour. Bull. SE-73*,U. S. Dep. of Agric., Southeast. Forest Exp. Stn., Asheville, NC, 1984.

Stull, R.B., *An Introduction to Boundary Layer Meteorology*, Kluwer Academic, Norwell, Mass., 1988.

White, A., and C. Fairall, Convective boundary layer structure observed during ROSE-I using the NOAA 915 Mhz Radar Wind Profiler, *NOAA Tech. Memo., ERL WPL-205*, Environ. Res. Lab., Boulder, Colo., 1991.

Zimmerman, P., J. Greenberg, and C. Westberg, Measurements of atmospheric hydrocarbons and biogenic emission fluxes in the Amazon Boundary Layer, *J. Geophys. Res., 93*, 1407-1416, 1988.

Zimmerman, P., Testing of hydrocarbon emissions from vegetation, leaf litter and aquatic surfaces, and development of a method for compiling biogenic emission inventories, *Publ. EPA-450-4-70-004*, U.S. Environ. Prot. Agency, Research Triangle Park, N.C., 1979.

---

G. Allwine and H. Westberg, Department of Civil and Environmental Engineering, Washington State University, Pullman, WA 99164.

K. Davis, J. Greenberg, A. Guenther, L. Klinger, W. Pollock, and P. Zimmerman, National Center for Atmospheric Research, P.O.Box 3000, Boulder, CO 80307.

C. Ennis, National Oceanic and Atmospheric Administration and Cooperative Institute for Research in Environmental Sciences, Boulder, CO 80303.

C. Geron, Office of Research and Development, U.S. Environmental Protection Agency, Research Triangle Park, NC 27711.

(Received January 16, 1995; revised September 10, 1995; accepted September 10, 1995.)